

DARK CURRENT STUDIES FOR SWISSFEL

F. Le Pimpec, R. Zennaro, S. Reiche, E. Hohmann, A. Citterio, A. Adelman
 Paul Scherrer Institut, 5232 Villigen, Switzerland
 B. Grigoryan
 CANDLE Yerevan, Armenia

Abstract

Activation of the surroundings of an accelerator must be quantified and those data provided to the official agencies. This is a necessary step in obtaining the authorization to operate such an accelerator. SwissFEL, being a 4th generation light source, will produce more accelerated charges, which are dumped or lost, than conventional 3rd generation light source, such as the Swiss Light Source. We have simulated the propagation of a dark current beam produced in the photoelectron gun using tracking codes like ASTRA and Elegant for the current layout of SwissFEL. Experimental studies have been carried out at the SwissFEL test facilities at PSI (C-Band RF Stand and SwissFEL Injector Test Facility), in order to provide necessary input data for detailed study of components (RF gun and C-band RF structures) using the simulation code OPAL. A summary of these studies are presented.

DARK CURRENT SIMULATIONS FOR SWISSFEL

In an RF gun, the dark current is initially generated by field emission from the photocathode and around the irises of the cavities for all accelerating RF structures. The direction of propagation of the electrons obviously depends on the RF phase and the efficiency of propagation depends of the type of cavity, traveling or standing wave (TW, SW). Impinging electrons to the surrounding walls of the cavity can produce secondaries. Those secondary electrons can also be captured and transported along the beam line and add to the dark current.

ASTRA simulations

We have simulated the dark current of the SwissFEL [1] S-band standing wave photogun to the end of the second 4 m long S-band traveling wave structure, by using the tracking code ASTRA [2]. The initial electron bunch was produced by using the SwissFEL nominal bunch, spreading its dimension in time and space. The emission time was limited to 120 ps which only covers one RF bucket $\pm 60^\circ$ around the on-crest phase. We turned off the space charge option. The dark current is in reality emitted at some threshold and at every RF bucket. This simple approximation is sufficient as every other dark current bucket propagating downstream of the RF gun will be transported identically by the machine optics. From the initial 300 k particles of the bunch, $\sim 22\%$ are lost on the cathode. The losses on the walls (in percent) are quantified along the first 13 m of

the machine, Fig.1, using the remaining ~ 234 k particles. Only 9.7% of those remaining particles reach the beginning of the third S-band accelerating structures. As shown in Fig.1, more than 90% of the bunch is lost before even reaching the first S-band structure with a ~ 7 MeV kinetic energy. The 9.7% remaining particles are concentrated in the core of the initial bunch. The output distribution was reused as an input for the elegant tracker [3] starting from the beginning of the third S-band structure.

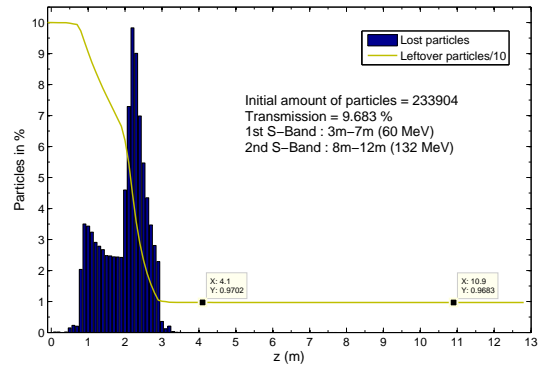


Figure 1: Histogram of the particle losses at the walls of the accelerator up to the end of the second S-band cavity (132 MeV). The continuous line represents the surviving particles in percent (/10) of the initial remaining particles.

Elegant simulations

The leftover particles from the ASTRA simulation were not numerous enough to do a proper elegant simulation. We have multiplied the input distribution by cloning every particle with a small change in their positions and momenta. We hence produced 2.2 million particles. The tracking was done using the SwissFEL Elegant model which includes the physical apertures of the machine and by adding collimators toward the end of the Aramis beam line [1]. The space charge and wake field options were turned off. Fig.2 (bottom plot) and Fig.3 show the location where particles are lost and with which energy and energy spread. The energy spread for the lost particles is small, less than 1%, as can be seen by the small error bars displayed in the bottom plot of Fig.2. Losses are concentrated before the first bunch compressor ($s \sim 50$ m) and at the second bunch compressor ($s \sim 200$ m), as shown in Fig.3. No other losses are recorded after the second bunch compressor. The transverse collimators placed at the end of the

machine ($s > 400$ m) induce dark current losses only for apertures smaller than 2 mm in radius.

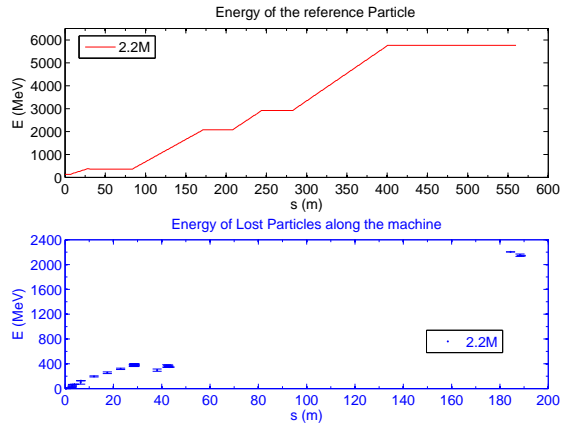


Figure 2: Top: Energy gained by the reference particle up to the end of the Aramis beam line. Bottom: Average energy and the standard deviation of the energy of the lost particles along the machine.

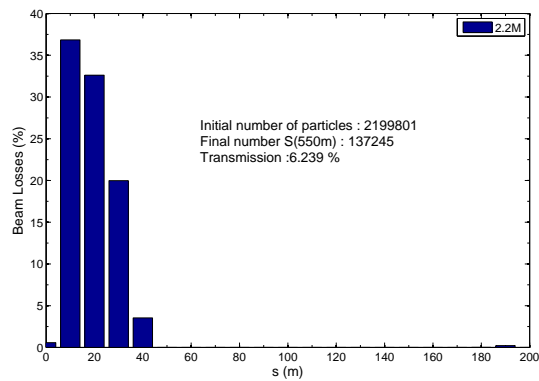


Figure 3: Histogram of the particle losses at the walls of the accelerator up to the end of the Aramis beam line (6 GeV)

Further simulations were carried out to find out the effects of different acceleration schemes on losses, due to potential SwissFEL operation conditions. The case presented in Fig.2 and 3 uses the full acceleration in LINAC 3 up to ~ 6 GeV. LINAC 3 is the last stage of acceleration for the hard X-ray beamline. It raises the beam energy from ~ 3 GeV to 6 GeV. This linac starts downstream of the beamline switchyard at $s \approx 280$ m. More details about the layout of the machine can be found in reference [1]. The other cases schemes simulated were the following.

- * Acceleration in LINAC 2 to 3 GeV and deceleration to 2.1 GeV before the entrance in LINAC 3.
- * Acceleration in LINAC 2 to 3 GeV and deceleration to 2.1 GeV using the last C-band structures at the end of LINAC 3.

- * Acceleration in LINAC 3 to 3.5 GeV and deceleration to 2.1 GeV using the last C-band structures at the end of LINAC 3.

They show no differences in losses for the same aperture of the collimators as the case presented here. Small differences arose for collimator sizes below the 2 mm radius.

Finally, we used elegant to track back some potential dark current produced by the TW C-band RF structures [4]. In a TW structure the RF capture phase exists only in the direction of propagation of the RF wave. Due to the design of our C-band structure, we do not expect any dark current above a few MeV traveling upstream of the LINAC. In elegant reversing the linac model will also reverse the direction of propagation of the RF hence allowing capture of an upstream propagating electron beam. Despite this limitation, we find that no dark current produced by the last C-band structure of LINAC 3 makes it back to the beginning of the machine for an initial electron energy below 25 MeV. This energy exceed by far the energy gained by electrons accelerated through 2 or 3 cells in a structure.

OPAL simulations

The preceding simulations have been carried out by using a blown up bunch based on the initial SwissFEL bunch. In order to use a more adequate bunch distribution, we have used the dark current simulation capabilities of OPAL [5, 6], turning off the secondary electron emission switch. We have tested the emission and propagation of a dark current beam using a Fowler-Nordheim (FN) threshold for emission of 40 MV/m and a FN enhancement factor β of 80. For the component simulation, we have used the actual layout of the SwissFEL injector test facility gun, labeled CTF3 in Fig.4 [7]. The CTF3 gun is a two and a half cell SW RF structure. The RF peak field at $t=0$ ps is 100 MV/m on axis. For every picosecond the RF phase changes by 1° . The electrons are created at first on the cathode side and on the downstream side of the irises and electrons start propagating downstream of the beam line. 180° later the electrons are created in the upstream side of the irises and start propagating upstream (toward the cathode). Fig.4 shows a snapshot at $t=545$ ps of the propagation of the electrons. The 6D phase space output of the simulation can be used as an input for the OPAL or elegant trackers. The modified module also handles TW structures. We plan to simulate the dark current production and propagation from an actual C-band test structure [4].

EXPERIMENTAL RESULTS AT VARIOUS SWISSFEL FACILITIES

Dark current at the SwissFEL injector

In order to provide proper inputs for the simulation we measured the dark current produced by the injector RF photogun (CTF3), and by the 4 m long S-band TW structure. Its propagation along the beamline was also studied [7].

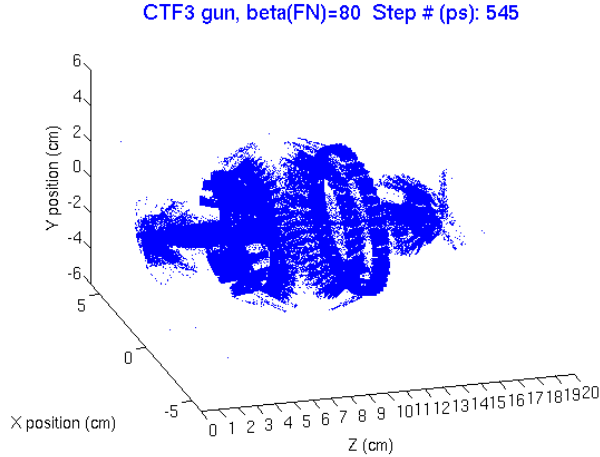


Figure 4: Propagation of the dark current in a SW photogun. The electron propagates upstream toward the cathode and downstream toward the exit of the gun

The CTF3 gun produces around 6 nC of dark current at nominal power (100 MV/m accelerating gradient). The charge is measured using the wall current monitor (WCM) located downstream of the gun. A second WCM is available downstream of the bunch compressor (BC). The emission of dark current in the gun is FN driven, as shown by the left plot in Fig.5. Using equation 1 in [8], we have extracted the FN enhancement factor $\beta = 78$ for such structure, Fig.5 (right plot),

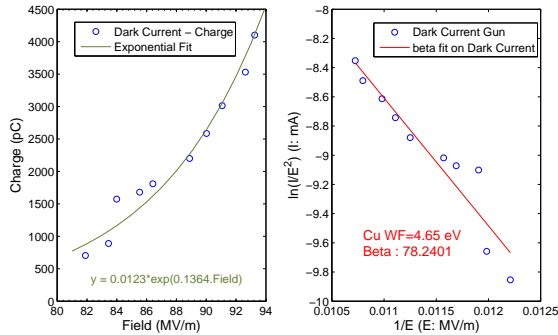


Figure 5: Left: CTF3 gun charge emission vs accelerating field. Right: Enhancement factor β determination.

$$\beta = \frac{6.83 \cdot 10^3 \times \Phi^{\frac{3}{2}}}{k_2} \quad (1)$$

where $\Phi = 4.65 \text{ eV}$ is the work function, and k_2 is the slope of the fit. Warm RF cavities with β of ~ 50 are usually consider good structures.

In order to determine the energy spread of the dark current we have used two techniques. In one case, we have varied the input power at the gun and looked at the beam at the screen located at the dump of the energy spectrometer. In the other case, we swept the beam on the screen using

the spectrometer dipole at nominal power. We measured a threshold for dark current at 4.3 MeV and a maximum energy of 7.2 MeV. The dark current energy on the lowest end could be lower than the measured 4.3 MeV, but we could not detect any electrons neither on the WCM nor on any scintillating screens of the beamline. The dark current emitted by the gun was measured, by the use of a WCM, to be 6 nC increasing by a couple of nC over time (months). The transmission of this dark current through the injector accelerator (5%) is in agreement with elegant simulations (6%, Fig.3).

We have tried to observe the dark current emitted solely by the TW S-band structures, running at 28 MW of input power (17 MV/m), on the upstream and downstream screens of each structures. No dark current was detected. A gamma ray spectrometer, facing the second S-band structure at a distance of 1 m and then 30 cm, showed no signal during the S-band operation. From these series of experiments, we concluded that the dark current measured downstream of the bunch compressor (300 pC) came solely from the gun dark current.

Off-line radiation measurements performed at the injector were in qualitative agreement with the ASTRA results. On-line radiation measurements show a significant high dose rate (normally given in terms of ambient dose equivalent) at the entrance of the fourth TW S-band structure (FINSB04), instead of the first one, and at the entrance of the BC (BC.Front), Fig.6. This seems contradictory to the simulations results, but one has to take into consideration the energy of the particles at FINSB04 and at the entrance of the first S-band structure (FINSB01). More electrons are lost at 7 MeV, entrance of FINSB01, than at 200 MeV, entrance of FINSB04, but the radiation production for electrons with an energy of 200 MeV is higher than at 7 MeV. Photon and neutron dose rate (in arbitrary units) is produced by the losses of the dark current on the accelerator chamber wall, Fig.6. The results are normalized to the highest measured dose rate arising from neutrons. At this point, the absolute data values (in terms of ambient dose equivalent) are under scrutiny. The detectors used are calibrated for a continuous radiation emission and not for radiation produced by a machine running at 10 Hz. The top plot, in Fig.6, shows the dose rate produced when the machine is accelerating the electron beam produced by the laser to 230 MeV and the dark current. The bottom plot shows solely the radiation produced by the dark current (laser is OFF). The contribution to the dose rate by the losses of electrons from the SwissFEL electron beam is negligible compared to the dark current produced by the gun. In addition, and not shown here, when the gun RF and the laser are turned off, the dose rate measured is close to background in most sections of the machine and of a few percent near the BC.

In order to reduce the radiation dose produced by lost electrons from the dark current, we have inserted an aperture at the location of the first screen. It is located downstream of the first WCM and before the first BPM. The

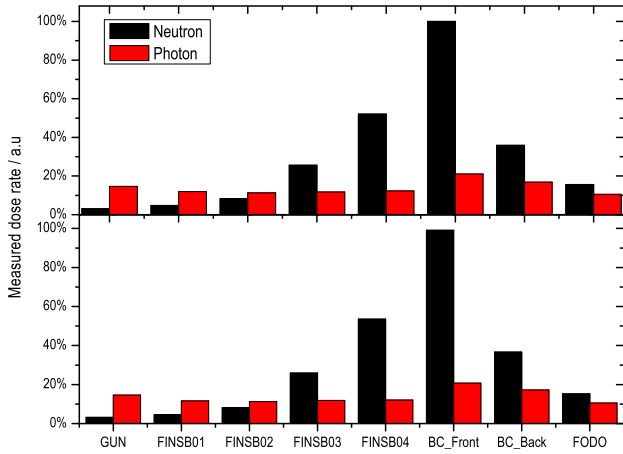


Figure 6: Measured radiation dose rate in arbitrary units along the machine measured 1 m away from each component. The dose rate is normalized to the highest measured value. Above : Laser is ON and all RF components are ON. Below : Laser is OFF and all RF components are ON

second WCM, downstream of the BC, does not record any dark current when this aperture is introduced in the beam line. Concurrent radiation dose measurements are currently under analysis.

Overall, on-line radiation and dark current measurements are in qualitative agreement with Elegant simulation results performed using SwissFEL's injector layout [1].

Dark current of a C-band test structure

The main acceleration of SwissFEL will be provided by C-band structures with an RF klystron pulse of 350 ns flat top and an on-axis maximum gradient of 28 MV/m [1]. It is of importance to test not only the quality of the mechanical production of such structures, but also their RF properties [4]. Two small prototypes have been RF tested, with a repetition rate of 10 Hz for the first structure and 100 Hz for the second one. Their dark currents were measured using the two Faraday cups (FCs) installed at each end of the beamline Fig.7. For the future structures an Integrated Current Transformer (ICT) [9] will be installed in the beamline.

We did not record any dark current on either the upstream or downstream FCs while running the C-band cavity for many hours at an accelerating gradient of 38 MV/m, hence 10 MV/m above the design value, and with a 350 ns RF flat top pulse. This amounts to ~ 51 MW of input power. The second C-band structure is currently RF tested with a flat top pulse already exceeding 500 ns. In both cases, dark current was detected solely on the Faraday cups during breakdowns. The breakdown rate is shown, Fig.8, for the second C-band structure for various accelerating field and pulse length. The data were obtained after various conditioning hours at different pulse length and RF power hence the discrepancy observed at 1 μ s. The lowest point at 1 μ s has been obtained before the dismantling of the test Struc-

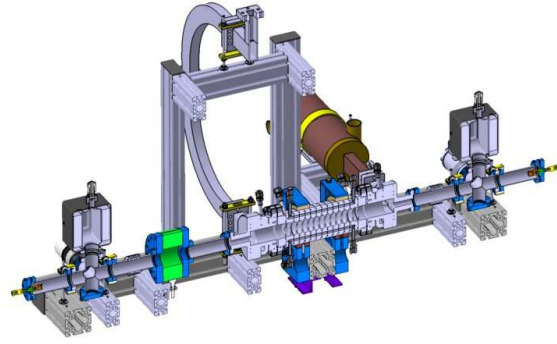


Figure 7: C-Band TW structure test stand, showing a faraday cup at each end of the beam line and an ICT.

ture #2. This shows the effect of a good conditioning.

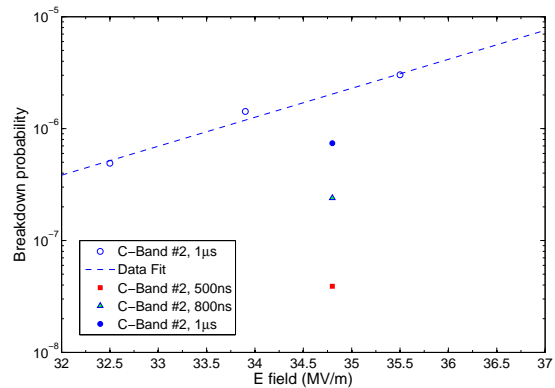


Figure 8: Breakdown probability of a C-band structure running at 100 Hz repetition rate for various RF pulse length and accelerating gradient.

The use of an X-ray scintillator [10], placed 1 m away from the structure, proves that dark current exists inside the structure. Using the NIST [11] database, we determined that photons > 300 keV can make it through 40 mm of Cu. At 38 MV/m on axis field, an electron in 1 cell (2 cm) can acquire up to 750 keV. The X-ray data are well fitted by the use of an exponential function, as expected for dark current coming from field emission, Fig.9.

Using equation 1 and assuming that the integrated x-ray signal is proportional to the dark current, we estimated that the FN β is 68 (350 ns long pulse). This value is consistent for the two structures tested. The evolution of the FN β was also recorded after a major breakdown. β peaked to 150 and diminished to 65 after hours of conditioning.

CONCLUSIONS

In order to obtain the necessary official authorization to operate SwissFEL, the production of radiation along the machine must be quantified. We have produced a first set of simulation results using ASTRA, Elegant and OPAL as

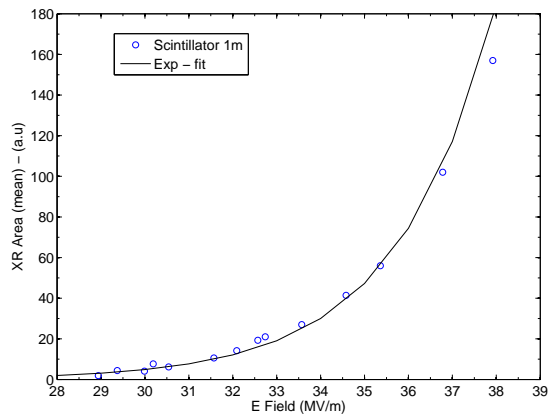


Figure 9: X-ray signal in function of the Electric Field inside the C-Band TW structure. The curve shows a FN type electron emission.

well as carrying out measurements at two SwissFEL facilities. The outcomes are :

- * Like in many other facilities around the world, the dark current is essentially produced by the SW photogun.
- * From simulations: most of the dark current is lost at the first S-band structure.
- * The remainder of it is mostly lost before the first bunch compressor.
- * Qualitative and comparative online radiation measurements show a low dose rate at the first S-band structure (unexpected), a high dose rate at the fourth S-band structure (unexpected) and a high dose rate at the entrance of the BC (expected)
- * Only a small fraction of the dark current, mainly its core produced at the photocathode, goes to the end of SwissFEL.
- * The S-band structures do not produce any recordable dark current nor X-rays when running at nominal power.
- * At nominal power and pulse length, the C-band test structures produce no measurable dark current, although electrons are present in the structures (X-ray signal).

Finally, we are continuing the dark current investigation on subsequent C-band structures by installing an ICT closer to the exit/entrance of the structure. We will run OPAL using the C-band test structure geometry and use the X-ray data to benchmark the simulations. Following the radiation measurements and simulations results, the SwissFEL layout infrastructure (air vents and shielding) is undergoing some modifications.

ACKNOWLEDGMENTS

We would like to thank A. Jurgens for his help at the C-band test facility. The lead author is indebted to his beam dynamic colleagues for their various help. We also acknowledge the help of C. Wang (CIAE, China) for modifying OPAL according to our needs. We also thank the radiation protection group for their support of this work.

REFERENCES

- [1] R. Ganter, editor. *SwissFEL Conceptual Design Report*. PSI-10-04. 2012.
- [2] K. Flöttmann. A Space Charge Tracking Algorithm. <http://www.desy.de/~mpyflo/>.
- [3] M. Borland. *Elegant: A Flexible SDDS-Compliant Code for Accelerator Simulation*. Advanced Photon Source LS-287, September 2000.
- [4] R. Zennaro, J. Alex, H. Blumer, M. Bopp, A. Citterio, T. Kleeb, L. Paly, J.-Y. Raguin. Design Construction and power conditioning of the first C-band accelerating structure for SwissFEL. In *IPAC12, New Orleans, USA, 2012*.
- [5] A. Adelman, C. Kraus, Y. Ineichen, J. J. Yang. The OPAL (Object Oriented Parallel Accelerator Library) Framework. Technical report, PSI-PR-08-02, 2008. http://amas.web.psi.ch/docs/opal/opal_user_guide.pdf.
- [6] C. Wang, A. Adelman and Y. Ineichen. A Field Emission and Secondary Emission Model in OPAL. In *HB2010, Morschach, Switzerland, 2010*.
- [7] M. Pedrozzi, editor. *SwissFEL Injector Conceptual Design Report*. PSI-10-05. 2010.
- [8] F. Le Pimpec, C. Gough, V. Chouhan, S. Kato. Field emission from carbon nanotubes in DC and pulsed mode. *Nuclear Instruments and Methods in Physics Research A*, 660:7–14, 2011.
- [9] Bergoz Instrumentation. <http://www.bergoz.com/>.
- [10] F. Le Pimpec et al. Results of the PSI Diode-RF Gun Test Stand Operation. In *IPAC2010, Kyoto, Japan, 2010*.
- [11] <http://www.nist.gov/pml/data/xray-gammaray.cfm>.